Hindawi
Geofluids
Volume 2020, Article ID 1865326, 18 pages
https://doi.org/10.1155/2020/1865326

Research Article

Case Study: In Situ Experimental Investigation on Overburden Consolidation Grouting for Columnar Jointed Basalt Dam Foundation

Jinxi Dou,[1,2] **Mengxia Zhou**,[3] **Zhilin Wang**,[3] **Kexiang Wang**,[3] **Shui Yuan**,[4] **Mingqiang Jiang**,[4] **and Guijin Zhang**[1,2]

[1]*School of Hydraulic Engineering, Changsha University of Science & Technology, Changsha, 410114 Hunan, China*
[2]*Key Laboratory of Water-Sediment Sciences and Water Disaster Prevention of Hunan Province, Changsha, 410114 Hunan, China*
[3]*China Three Gorges Projects Development Co., Ltd., Chengdu, 610000 Sichuan, China*
[4]*Sinohydro Bureau 8 Co., Ltd., Changsha, 410114 Hunan, China*

Correspondence should be addressed to Guijin Zhang; gjzhang84@126.com

Received 11 October 2019; Revised 27 December 2019; Accepted 3 January 2020; Published 24 February 2020

Academic Editor: Constantinos Loupasakis

The dam foundation rock mass, at the Baihetan hydropower station on the Jinsha River, is mainly columnar jointed basalt, with faults and fissures developed. Considering adverse factors such as the unloading relaxation or the opening of the fissures due to excavation blasting, consolidation grouting is needed to improve the integrity of the dam foundation rock mass. According to the physical and mechanical properties of columnar jointed basalt and the continuity of construction, the effectiveness of overburden consolidation grouting is experimentally studied. The results show that this grouting technology can obviously improve the integrity and uniformity of a dam foundation rock mass and reduce the permeability of the rock mass. After grouting, the average increase in the wave velocity of the rock mass is 7.3%. The average improvement in the deformation modulus after grouting is 13.5%. After grouting, the permeability of 99% of the inspection holes in the Lugeon test section had Lugeon values of no more than 3 LU. This improvement is considerable and provides a case to engineering application.

1. Introduction

The safe operation of arch dam depends on the safety of dam foundation, dam structure, hydraulic device, and reservoir water environment. The foundation of arch dam is subjected to huge hydraulic thrust during normal operation. China has built many dams, but with the development of science and technology and the improvement of engineering technology, many dams have been built under complicated geological conditions [1]. The Xiaowan hydropower station, Xiluodu hydropower station, and the 180-meter-high Katse hyperbolic arch dam in Lesotho are all built on basalt. However, the basalt of Baihetan arch dam site is more complex. The basalt at Baihetan dam site is characterized by irregular and undulated columnar joints, irregular and incomplete cylinder section, low development of implicit fractures and low deformation modulus, development of shear belts, low deformation and shear strength, and cleavage density in some lithologic segments [2]. Columnar joints and microfissures in fresh columnar jointed basalts are rigid structural surfaces, closed under confining pressure, easy to open, and relax after releasing confining pressure [3–18]. It cannot meet the requirement of sufficient bearing capacity and stability of dam foundation rock mass as arch dam. In order to increase the deformation resistance of the foundation, improve the shear and seepage resistance of the structure surface, avoid the foundation surface bedrock unloading relaxation, reduce the impact of excavation blasting crack surface opening, and improve the integrity of the dam foundation rock mass, it is necessary to carry out consolidation grouting test for dam foundation, study and prove the feasibility and reliability of rock mass as the foundation of arch dam after grouting, and provide reference for reasonable design and determination of construction parameters of rock mass consolidation

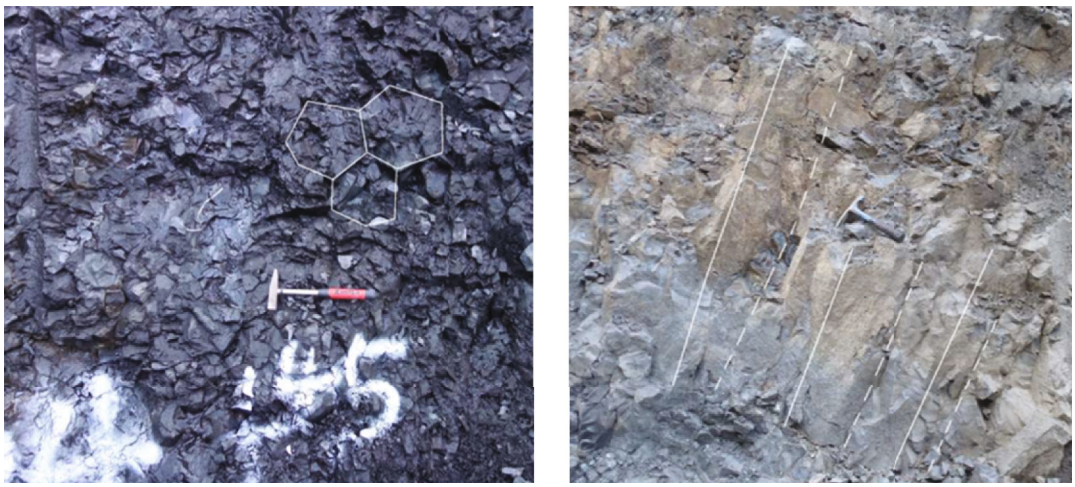

Figure 1: Small-scale columnar jointed basalt and weakly weathered columnar jointed basalt [15].

grouting in dam area. Typical type I basalt columnar joints are shown in Figure 1.

Some scholars have studied the seepage prevention technology of dam foundation reinforcement for different rock masses. Wu et al. [19] studied the deformation of the basalt foundation of the Xiluodu arch dam. The deformation of the dam foundation rock mass during excavation was continuously monitored, and it was concluded that there was no long-term unloading deformation of the dam foundation rock mass. Fan et al. [20] found that when the Katse hyperbolic arch dam constructed on basalt was excavated to the riverbed, buckling of the basalt layer and soft brecciated layer occurred due to the high horizontal stress. Develay et al. [21] studied the construction of the main dam of the Baise Water Conservancy Project on diabase dykes and used grouting to reinforce the slightly weathered rock masses. Homas and Thomas [22] conducted field and laboratory tests on grouting in a fractured rock mass and obtained a better understanding of grouting pressure and grouting materials. Zhao [23] used chemical grouting and concrete replacement methods to treat the weak rock layers in the foundations of the Ertan and Shapai hydropower stations. In addition, Li and Tang [24] studied rock anchoring and grouting. Karl [25] studied the use of flake granite as a dam foundation. Turkmen et al. [26] used grouting to address the seepage problem of the karst limestone foundation of the Kalecik dam (southern Turkey) and built a grouting curtain 200 m long and 60 m deep along the dam. Kikuchi et al. [27] studied the improvement in the mechanical properties of dam foundations by consolidation grouting of the corresponding rock mass and concluded that grouting can improve the uniformity and deformation of rock masses. Salimian et al. [28] studied the influence of grouting on the shear characteristics of rock joints, and the results showed that grouting had a positive impact on the shear strength of rock. With the decrease in the water-cement ratio, the compressive strength of a cement slurry increases, but its shear strength does not necessarily increase.

In previous studies, it can indicate that the columnar jointed basalt is rarely reported as the engineering case of high arch dam foundation, and there are also few scholars to carry out research on the reinforcement technology of columnar jointed basalt as the foundation of arch dam. Columnar jointed basalt used as the foundation of a high arch dam is rarely reported. Due to the existence of the columnar joints and under the combined action of the strike, dip, and in situ stress, shear deformation often occurs along the excavation face with the increase in excavation depth. To increase the deformation resistance of the foundation, reduce the impact of excavation blasting-induced crack surface opening of the dam foundation and also to improve the permeability resistance of the structural surface and the integrity of the dam foundation rock mass. According to the physical and mechanical properties of columnar jointed basalt, which require thorough research, a method of overburden consolidation grouting is adopted to reduce the dam foundation rock mass and foundation excavation unloading rebound and damage. Additionally, columnar joints in shallow basalt are opened by the stress relaxation, and it also solves the cracking problem of using concrete cover grouting [29–31], effectively improving the deformation resistance and the permeability resistance of the structural plane under shear; furthermore, this approach is suitable for use during the continuous construction of high arch dam foundation.

2. Project Overview

2.1. Project Summary. The Baihetan hydropower station is located in Ningnan County, Sichuan Province, and Qiaojia County, Yunnan Province, downstream of the Jinsha River, a major tributary of the Yangtze River. The station is connected with the Wudongde hydropower station and adjacent to the Xiluodu hydropower station. The location of the Baihetan hydropower station is shown in Figure 2.

The barrage is a concrete double-curved arch dam with a dam top elevation of 834 m, maximum dam height of 289 m, arch roof thickness of 14.0 m, maximum arch end thickness of 83.91 m, including the maximum thickness of the expanded foundation of 95 m. The arc length of the dam top is approximately 209.0 m, divided into 30 transverse

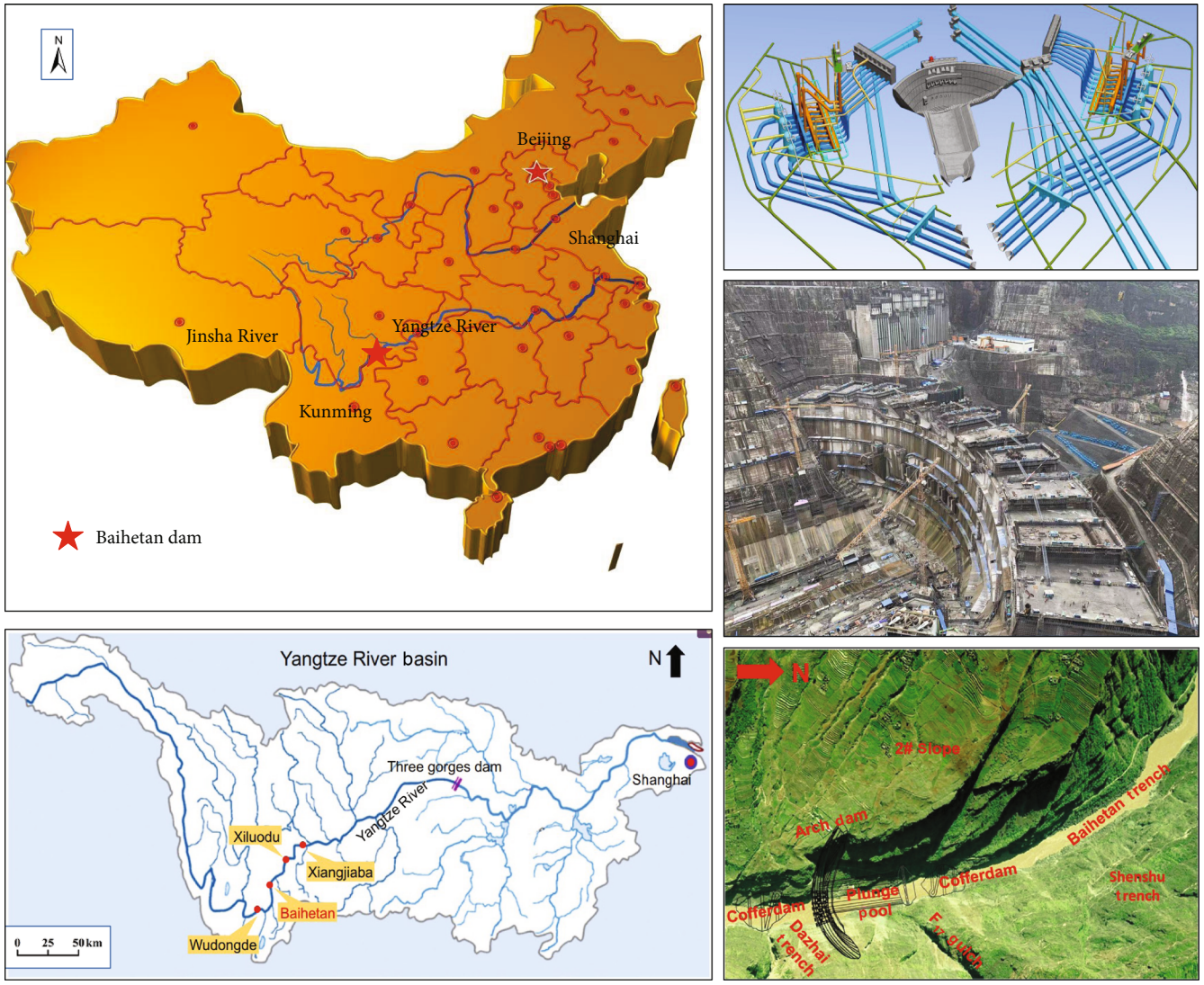

Figure 2: Baihetan hydropower station located in China [15].

joints, and there are 31 dam sections. The concrete cushion is set above an elevation of 750.0 m, and the base of the dam section is expanded, but no longitudinal joints are set in the dam. The normal water level of the reservoir is 825 m, and the total storage capacity of the high reservoir is 20.627 billion m^3. The installed capacity of the power station is 16000 MW, with an average annual generating capacity of 62.521 billion kWh.

2.2. Engineering Geology of the Right Bank

2.2.1. Formation Lithology. The bedrock in the dam site is mainly basalt ($P_2\beta_3$~$P_2\beta_6$) of the Emeishan formation, which is mainly composed of microcrystalline and cryptocrystalline basalt, followed by porphyritic basalt with almond-shaped crystals, with interbedded basaltic brecciated lava and tuff. The columnar joints in this basalt create different column sizes and lengths, which can be divided into three types according to their developmental characteristics (see Table 1). Basalts and Quaternary alluvial layers are mainly exposed at the dam foundation below 600 m on the right bank. Layers of basalt with almond-shaped pores outcrop from $P_2\beta_3^4$ above an elevation of 590 m; in $P_2\beta_3^{3\text{-}4}$, layers of cryptocrystalline basalt outcrop at an elevation of 590~580 m and below an elevation of 580 m; in $P_2\beta_3^3$, layers of type I columnar jointed basalt with column diameters of 13~25 cm and microfractures developed within the columns.

Below an elevation of 545 m, the $P_2\beta_3^{2\text{-}3}$ layer is breccia lava. In $P_2\beta_3^3$, columnar basalts with column diameters of 13~25 cm are mainly exposed in the right bank of the dam foundation. Above $P_2\beta_3^3$ are layers of $P_2\beta_3^{3\text{-}4}$ cryptocrystalline basalt. The overburden of the riverbed is sand, pea gravel, and bleached stone. The thickness of the dam foundation ranges from 11.8 m to 26.85 m, and the elevation of the lowest bedrock roof is 552.41 m. The basement rock mass is mainly composed of the first type of columnar basalt at the bottom of the $P_2\beta_3^3$ layer and the brecciated lava of the $P_2\beta_3^{2\text{-}3}$ layer. The underlying rock mass is the second type of columnar basalt in the $P_2\beta_3^{2\text{-}2}$ layer and the crystalline basalt in the $P_2\beta_3^{2\text{-}1}$ layer. The deep part (height up to 500 m) is brecciated

Table 1: Characteristics of columnar basalt in the dam site area of the Baihetan hydropower station.

Category	Column length (m)	Column diameter (cm)	Rock fragmentation (cm)	Distribution	Notes
Type I	2.0~3.0	13~25	5	$P_2\beta_3^2$, $P_2\beta_3^3$	
Type II	0.5~2.0	25~50	10	$P_2\beta_3^2$, $P_2\beta_6^1$, $P_2\beta_7^1$, $P_2\beta_8^2$	
Type III	1.5~5.0	50~250	—	$P_2\beta_2^2$, $P_2\beta_2^3$, $P_2\beta_4^1$	Incomplete cutting

lava at the $P_2\beta_3^1$ layer and cryptocrystalline basalt, porphyritic basalt, and crystalline basalt. The thickness of the brecciated lava in the $P_2\beta_3^{2\text{-}3}$ layer is 6.60~10.40 m, and the floor elevation is generally 550~520 m from left to right. The thickness of the columnar basalt in the second type of $P_2\beta_3^{2\text{-}2}$ layer is 25.70~27.70 m, and the floor elevation is generally 520~490 m from left to right.

2.2.2. Characteristics of Columnar Jointed Basalt. The cooling and contraction of magma is thought to have formed the columnar joints in the Baihetan dam area. Columnar jointed basalt is formed by chemical reactions of chlorite, kaolinite, epidote, and tremolite, and the fillings of columnar joints are dominated by chlorite. The dam site area hosts type I columnar jointed basalt with a high joint density, wide joint apertures, and undulating columnar joint surfaces that generally cut the rock into complete columns; the horizontal deformation modulus of this basalt is 9~11 GPa, and the vertical deformation modulus is 7~9 GPa. These rocks are grayish black and contain microfractures that are not throughgoing, in addition to the columnar joints. Columnar jointed basalts are cut into hexagonal or other irregular prismatic shapes and develop longitudinal and transverse microfissures at the same time, and there are many low-dipping structural planes in basalts. According to the quality classification of engineering geological rock masses, when the surface layer relaxes after unloading, the rock mass integrity is poor due to the fracture development.

2.2.3. Geological Structure. F_{14} and F_{16} are NW-trending steeply dipping faults, which cut the riverbed at an obtuse angle and are exposed on the downstream right side of the riverbed dam foundation. The riverbed develops only in bed C_2, which is deeply buried 120 m below the riverbed at the dam foundation, with an elevation below 430 m.

The dislocation zones RS_{331}, RS_{336}, RS_{3315}, VS_{333}, VS_{332}, etc. are in the exposed layer of the dam foundation, and the rest of the dislocation zones VS_{3210}, VS_{3215}, VS_{3216}, etc. are buried below the foundation. Except for RS_{336}, most of these dislocation zones are short, and most of them are distributed intermittently along the flow layer, allowing some connectivity along the flow layer. The distribution of the columnar basalt and shear zones is shown in Figure 3.

2.2.4. Ground Stress. The orientation of the maximum horizontal principal stress is nearly the E-W, which is nearly perpendicular to the river flow. The orientation of the minimum horizontal principal stress is approximately N-S. The rock mass within a range of 0~40 m below the bedrock surface (depth of 20~60 m) is in a relaxation state, which creates a stress relaxation zone with a maximum horizontal principal stress of 3~6 MPa. The range 40~70 m below the bedrock surface (depth of 60~90 m) exhibits increased stress, with a maximum horizontal principal stress of 6~12 MPa, inducing a local stress concentration phenomenon. There is a stress concentration zone 70~130 m below the bedrock surface (approximately 90~150 m deep), with a maximum horizontal principal stress of 22~28 MPa and a minimum horizontal principal stress of 13~15 MPa.

The slope of the right bank hosts a partially unloaded rock mass, which is buried at a depth of 200 m. The maximum horizontal principal stress orientation is N-S, which is nearly parallel to the river flow, and the shallow surface is deflected toward a nearby mountain to the N to NE. The average maximum horizontal principal stress in the near-shore slope is approximately 6.0 MPa, and the average minimum horizontal principal stress is approximately 4.6 MPa. The first principal stress orientation is approximately N-S, with a moderate inclination angle of approximately 35°, and the magnitude is 7~11 MPa. The second principal stress orientation is S20°E, and the dip angle is moderate to steep. The third principal stress has the following properties: orientation, N80°W; inclination, 21°; magnitude, 5~7 MPa.

3. Grouting Material

3.1. Raw Material

3.1.1. Cement. 42.5R ordinary Portland cement produced by a cement company in Yunnan is used in this research. The cement fineness is less than 5% of the sieve allowance through an 80 μm square hole sieve. The performance meets the relevant requirements of the Chinese general Portland cement standard (GBl75-2007). The chemical constituents of the Portland cement used in this study are shown in Table 2. Initial set time is 155 min. Final set time is 235 min. 28 d compressive strength is 46.3 MPa.

3.2. Slurry Ratio and Particle Size. According to Chinese standard DL/T5148-2012 (Technical Specification for Cement Grouting Construction of Hydraulic Structures) and experts, consolidation grouting of the sequence hole I and sequence hole II section using ordinary Portland cement grout, wet-ground cement grout is used for the sequence hole III. The water-cement ratio (water-cement mass ratio) of the ordinary Portland cement slurry is tested in four levels (2 : 1, 1 : 1, 0.8 : 1, and 0.5 : 1). The water-cement ratio of the wet-ground cement slurry is tested in four levels (3 : 1, 2 : 1, 1 : 1, and 0.5 : 1). For the wet-ground cement method, according to Chinese standard SL578-2012 (Technical Code for Experiment and Application of Fine Wet-Ground Cement Grouting Material), wet grinding equipment from

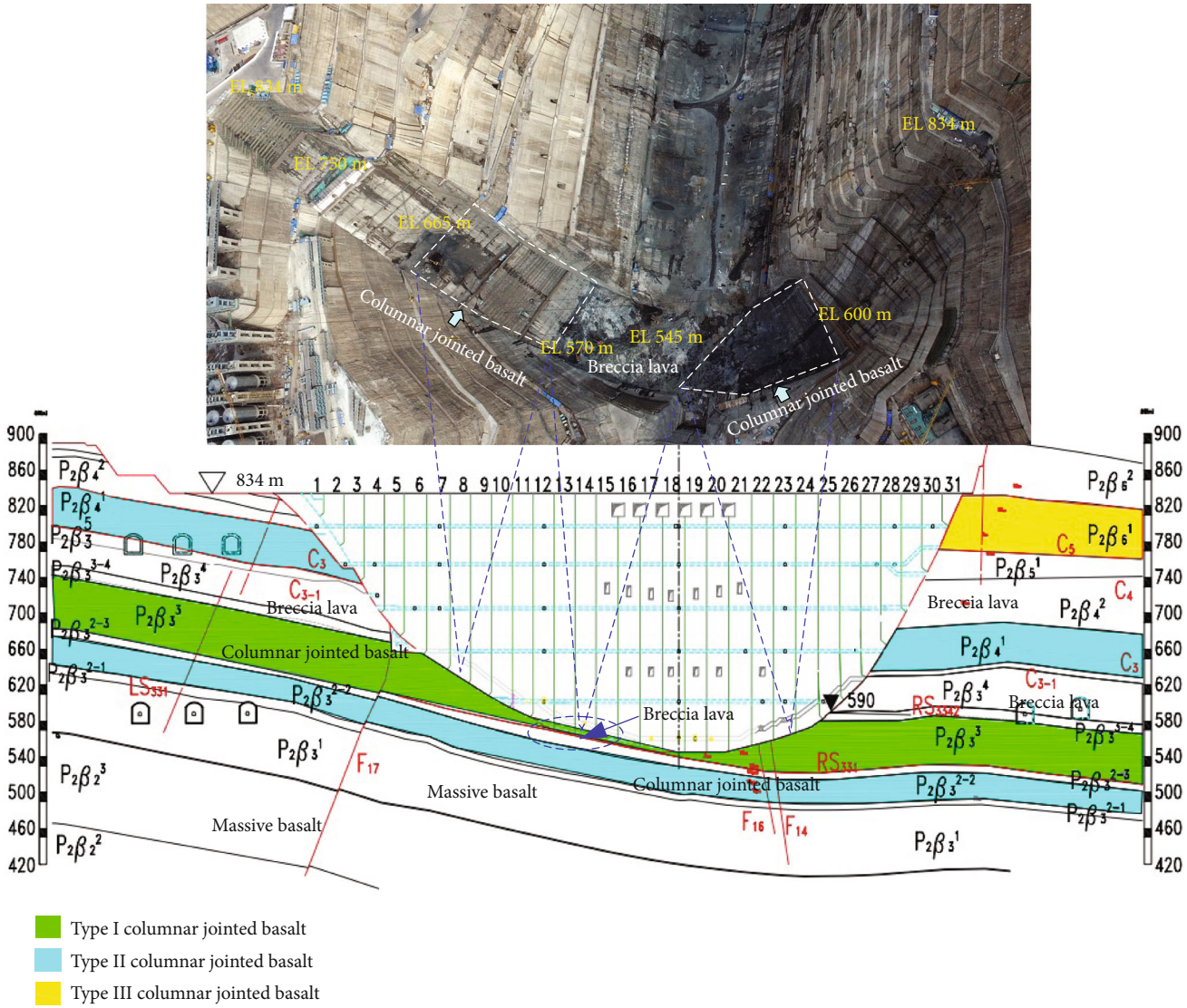

Figure 3: Geological condition of Baihetan hydropower station.

Table 2: The chemical constituents of the Portland cement used in this study.

Chemical constituents	SiO_2	Al_2O_3	Fe_2O_3	MgO	CaO	SO_3	Loss on ignition
Content (%)	22.3	7.1	4.5	2.4	56.6	2.2	2.5

the Wuhan Yangtze River Academy of Sciences Institute of Automation, instrument GJM–FII, was used for wet grinding. A sample was taken from cement that was ground three times (3~4 min each time) on site.

The particle size of the wet-ground cement was analyzed by using an NSKC-1 laser particle size analyzer, equipment from the Wuhan Yangtze River Academy of Sciences Institute of Automation. A particle size analysis of the wet-ground cement was conducted, and the results are shown in Figure 4. According to Figure 4, D95 (the maximum particle size with a cumulative mass distribution rate of 95%) = 37.46 μm, and D50 (average particle size) = 11.44 μm. According to the requirements of the specifications considered for wet grinding, after wet grinding, the cement particle size D95 (the maximum particle size with the cumulative mass distribution rate of 95%) ≤ 40 μm, and D50 (average particle size) = 10~12 μm. Thus, the data in Figure 4 shows that the cement after wet grinding meets the requirements of the specification. After sequence hole I or II grouting, rock fracturing decreases. According to the specification, the crack width is 0.1~0.5 mm in the rock mass after appropriate use of the wet-ground cement. The sequence hole III size can be

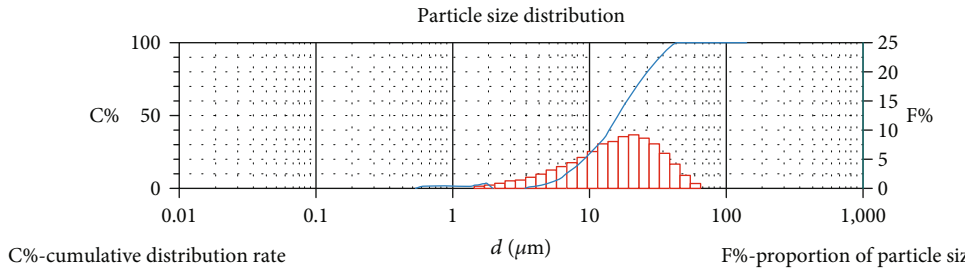

Figure 4: Particle size analysis of the wet-ground cement particles.

Table 3: Relationship between water-cement ratio (W/C) and the unit of slurry density.

W/C	3 : 1	2 : 1	1 : 1	0.8 : 1	0.5 : 1
Slurry density	1.21	1.30	1.53	1.62	1.85

Table 4: Relationship between water-cement ratio (W/C) and water drainage rate.

W/C	0.5 : 1	0.8 : 1	1 : 1	2 : 1	3 : 1
Drainage rate (%)					
Before grinding	15.3	22.5	27.2	54.1	81.2
After grinding	1.2	18.4	21.8	50.1	79.8

reduced because the wet-ground cement grain size is small and can improve the ability of the grout to flow into very small cracks. At the same time, to enhance slurry saturation, the water-cement ratio of the wet-ground cement is adjusted to 3 : 1, and the injection capacity of the slurry is increased by thinning the grout and reducing the particle size.

3.3. Slurry Performance

3.3.1. Slurry Density. Slurry density is the basis for calculating the total amount of grouting, and it is also an important index for adjusting the water-cement ratio of grouting. According to Chinese standard DL/T5148-2012 (Technical Specification for Cement Grouting Construction of Hydraulic Structures), a type 1002 mud density gauge is used to measure the slurry density. Slurry densities for different water-cement ratios are shown in Table 3. Table 3 indicates that as the water-cement ratio decreases, the slurry density increases, and the slurry also thickens. The density of the cement increases because the density of the water decreases.

3.3.2. Drainage Rate. According to Chinese standard DL/T5148-2012 (Technical Specification for Cement Grouting Construction of Hydraulic Structures), a 100 mL cylinder of cement slurry was measured under the weight of a volume of water that would accumulate due to 2 h of precipitation, and the ratio of that measurement to the initial slurry volume is called the drainage rate. The drainage rate can reflect the stability of a slurry to some extent. Table 4 shows that the drainage rate of the slurry with a water-cement ratio of 3 : 1 can exceed 80~90%, whereas the drainage rate of the slurry with a water-cement ratio of 1 : 1 is approximately 35%, indicating that most of the water in the thin grout that was injected into the cracks or holes in the rock during grouting drained out. However, the slurry drainage rate of the wet-ground cement is lower than that before grinding, and the lower the water-cement ratio is, the greater the decrease because of the adsorbability of cement particles. After wet grinding, the contact area of the cement with water increases, leading to a decrease in the water drainage rate. During an actual grouting process, slurry is injected into rock cracks under great pressure. Due to this high-pressure effect, the period for water analysis is shortened, and more water is squeezed out, so the particles are more densely packed, and the slurry strength is increased.

3.3.3. Compressive Strength of Consolidated Slurry. The early compressive strength of slurry in columnar basalt determines the ability of the grouting material to consolidate the dam foundation, while the late strength of consolidated slurry reflects the long-term stability of the grouting reinforcement. The strengths of the wet-ground cement slurry after 1 h of circulation under 5 MPa pressure and the ordinary cement slurry under normal pressure were measured. A concrete servo press is used to test the compressive strength of the consolidated slurry with a size of 70 mm × 70 mm × 70 mm for 7 d and 28 d. This test method is referred to as the cement sand strength test method (ISO method) (GB/T17671-1999). From Table 5, it can be concluded that the compressive strength of the consolidated wet-ground cement slurry is greater than that of the consolidated ordinary cement slurry of the same age and at normal pressure when the water-cement ratio is the same. Under high pressure, the compressive strength of the consolidated slurry is maximized when the water-cement ratio is 1 : 1. Under high pressure, the compressive strength of the wet-ground cement is greater than that of the consolidated ordinary cement slurry. These results show that under high pressure, the performance of the cement slurry is better than that under normal pressure, and the performance of the wet-ground cement is better than that of the ordinary cement.

4. Grouting Method

4.1. Test Position. The #25 dam section at an elevation of 609.76~590 m includes the permanent foundation plane and has the following properties: excavation slope ratio,

Table 5: Properties of the ordinary cement slurry and the wet-ground cement slurry under normal pressure and high pressure.

Property	Pressure	Variety of cement	3 : 1	2 : 1	1 : 1	0.8 : 1	0.5 : 1
7 d compressive strength (MPa)	Normal	Portland cement	3.25	4.10	5.40	7.63	11.60
		Wet-ground fine cement	4.21	7.3	12.3	14.5	15.4
	High	Portland cement	50.4	70.8	73.5	75.5	66.2
		Wet-ground fine cement	70.8	94.5	95.1	93.2	69.3
28 d compressive strength (MPa)	Normal	Portland cement	11.3	15.1	15.9	16.8	22.6
		Wet-ground fine cement	12.3	17.4	22.3	23.7	28.6
	High	Portland cement	83.4	99.6	102.2	101.6	86.5
		Wet-ground fine cement	105.8	108.7	111.6	109.7	95.3

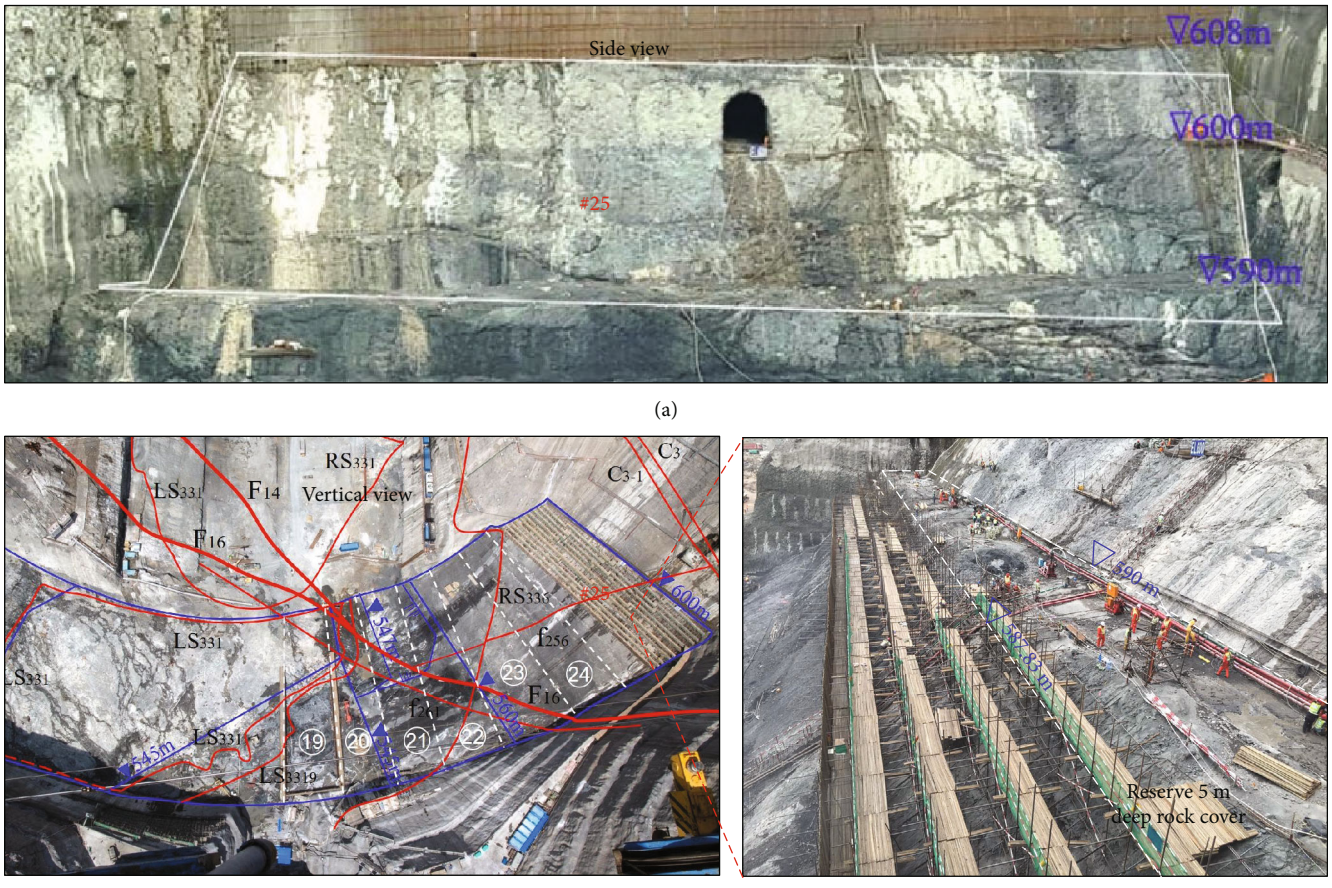

Figure 5: Location of overburden consolidation grouting in the #25 dam section.

1 : 0.79~1 : 1.27; strike N49°~52°W; top and bottom side length, 92.0 m and 94.8 m, respectively; slope length, 13.5~16.2 m; and area, 1367.7 m. Experts determined that a grouting test of the overburden of the dam foundation under the elevation of 590 m should be carried out in the #25 dam section on the right bank. The #25 dam section includes an 8 m wide road, elevation 590 m~587.83 m, an inclined surface, and a 5 m thick rock protection layer at the top, striking N49°W with an area of 857.8 m^2. Location of #25 dam section is shown in Figure 5.

4.2. Grouting Process. The process flow chart is shown in Figure 6, and some processes in the construction site are shown in Figure 7. The overburden consolidation grouting processes are shown below:

(1) Reserve 5 m overburden protection layer: reserve 5 m from the dam foundation surface for an overburden protection layer, adopting the hole closure method and 0.5 MPa pressure for the 5 m protection layer circulation grouting. When the injection rate is no more

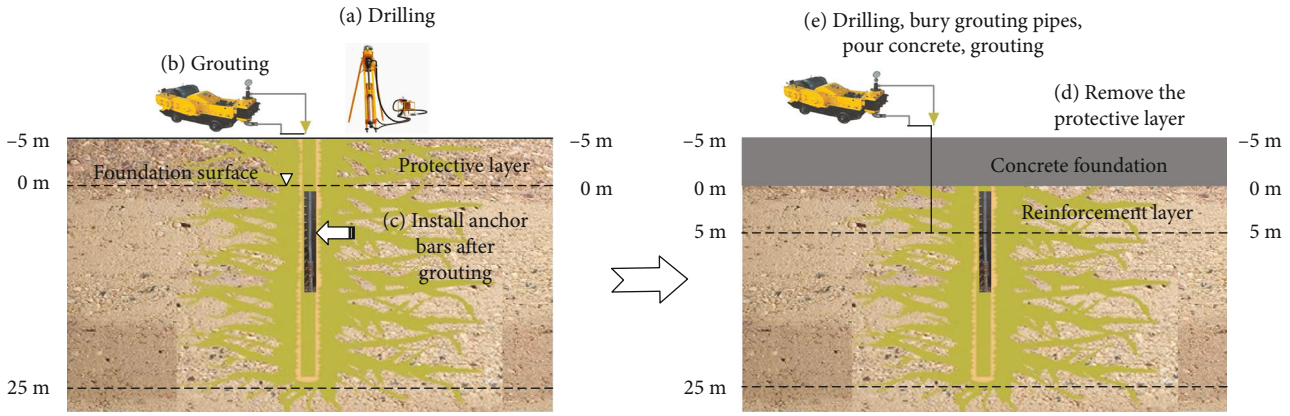

Figure 6: The overburden consolidation grouting processes.

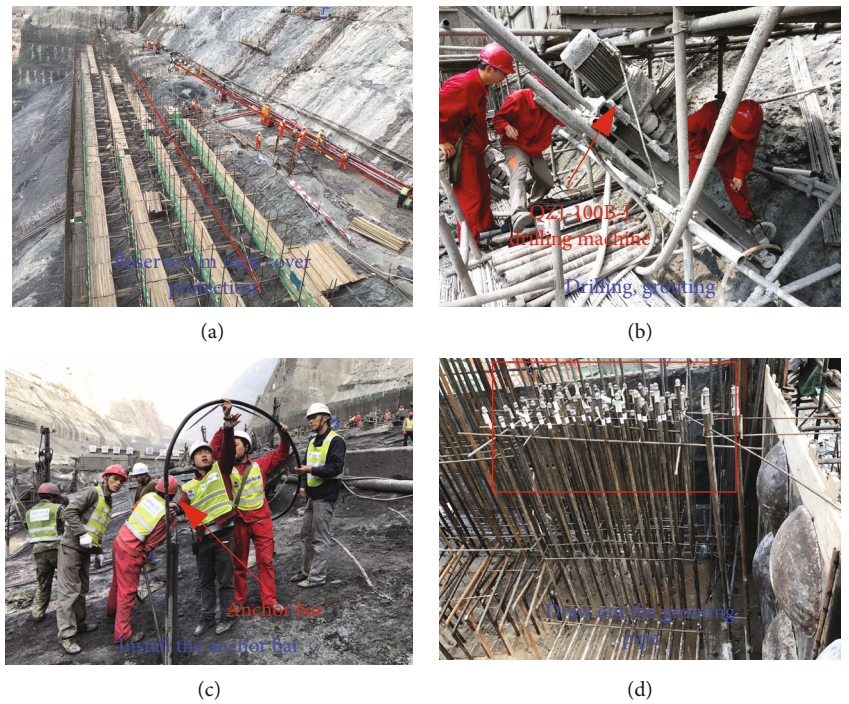

Figure 7: Construction technology of overburden weight section.

than 1.0 L/min, a hole can be drilled below the dam foundation surface

(2) Orifice closure, top-down segmented circulation grouting: the consolidation grouting below the dam foundation adopts segmented drilling, top-down injection, orifice closure, graded pressurization, and whole-section circulating grouting. When the injection rate is no more than 1.0 L/min, the grouting can be completed after 30 min of continuous injection

(3) The anchor bar pile: the adopted anchor bar is made of 3 anchor bars with a diameter of 32 mm and a single length of 12 m, which is placed 20 cm below the surface of the dam foundation grouting hole

(4) Excavation and removal of heavy cover: sallow blasting is performed on the protective cover of the rock, and mechanical excavation and blasting is performed to loosen the rock to the foundation plane

(5) Shallow tube: the next 5 m is used for grouting of the dam foundation surface between drilling pipe, from I to III sequence bore holes; the tube diameter of Φ110 mm, grouting pipe with a Φ38 mm steel tube, and slurry pipe with a Φ25 mm steel tube are used

(6) Tie the steel bar and pour concrete on the dam foundation

(7) Concrete cover repriming grouting: the grouting pressure of the priming pipe is 3.0 MPa, and the

Table 6: Consolidation grouting pressure and length in the test area.

Hole depth (m)	-5~0	0~5	5~10	10~15	15~20	20~25
I (MPa)	0.5	0.8~1.0	1.0~1.5	1.5~2.0	2.0~2.5	2.5~3.0
II (MPa)	0.5	1.0~1.5	1.5~2.0	2.0~2.5	2.5~3.0	2.5~3.0
III (MPa)	0.5	1.0~1.5	2.0~2.5	2.5~3.0	3.0	3.0

injection rate is no more than 1.0 L/min; then grouting can be completed

Regarding the technology of consolidation grouting to create a concrete cover, considering that high-pressure grouting leads to stratum lifting, tensile stress in the concrete, and concrete cracking, the overburden consolidation grouting technology is put forward. First, the 5 m protective layer of the rock mass is created by closed grouting, which can improve the grouting pressure of the rock mass below the foundation plane. Anchor bars are used to solve the problem of bedrock deformation. After the protective layer is removed, the monitoring data show that the blasting relaxation range is 0.2~2.2 m, with an average of 1.09 m. The surface relaxation problem is solved by using shallow primer pipe, creating a concrete cover in a timely manner, and applying later concrete cover reprimer pipe grouting. The problems of bedrock deformation, surface relaxation, consolidation grouting, and concrete construction interference are considered comprehensively. The completion of consolidation grouting before concrete pouring provides conditions for concrete pouring construction, which avoids the crossinterference of consolidation grouting and concrete construction and the problems of multiple entries and exits of the consolidation grouting equipment.

4.3. Slurry Transform. The sequence holes I and II use a water-cement ratio (mass ratio) of 2 : 1 in the initial grouting, whereas the sequence hole III uses a water-cement (wet-ground cement) ratio of 3 : 1 in the initial grouting. The grouting slurry is transforming from weak to strong step by step. This transformation follows the following principles:

(1) When the grouting pressure remains the same, injection rates should be reduced; or under a constant injection rate, when the pressure continues to rise, do not change the water-cement ratio

(2) When the injection amount of a grout of a certain grade exceeds 300 L, or the infusion time has reached 30 min, and the grouting pressure and injection rate have no significant change, the first-grade water-cement ratio of the grout should be changed to create a more concentrated grout

(3) When the injection rate is greater than 30 L/min, the grout can be thickened according to the specific construction conditions

4.4. Grouting Pressure. The consolidation grouting adopts the method of grading and pressurizing to reach the design grouting pressure by using an incremental approach. The relationship between the injection rate and pressure is strictly controlled during grouting so that no harmful lifting of the rock surface occurs due to the grouting and concrete. The grouting pressure of the protective layer is 0.5 MPa, and that of the first section below the foundation plane is 0.8~1.0 MPa. Later, the grouting pressure gradually increases by 0.5 MPa for each section. The maximum grouting pressure is 3.0 MPa, and the grouting pressure of the concrete guide pipe is 3.0 MPa (see Table 6). Standard for the end of grouting: the grouting operation can be considered completed when the injection rate of the protective layer section is no more than 1.0 L/min under the design pressure. In the sections below the protective layer, the injection rate is no more than 1.0 L/min under the design pressure, and the grouting operation can be completed after 30 min of continuous injection.

4.5. Grouting Hole Arrangement. The spacing of the consolidation grouting holes is 3.0 m × 3.0 m and 2.0 m × 2.0 m. The borehole is perpendicular to the foundation plane and penetrates 25 m below the foundation plane. The layout diagram of the consolidation grouting holes in the overburden is shown in Figure 8. The lifting dynamic monitoring hole, test hole, sequence hole I, sequence hole II, and sequence hole III are included. The test hole aperture is Φ76 mm; lifting dynamic deformation observation hole aperture, Φ91 mm. Because consolidation grouting holes need anchor bar piles, the consolidation grouting hole diameter is Φ110 mm. The tube grouting is injected through a steel pipe, with a head diameter of Φ38 mm, auxiliary diameter of Φ25 mm, and tube wall thickness of 1.5 mm. A QZJ-100B-J drilling rig was used to drill the grouting hole. All grouting holes are rinsed with a water pressure of 1 MPa to clear out the cracks. The flushing method utilizes open flushing, which flushes a large amount of water from the bottom of the hole to the area around the hole, and rotation flushing. The condition for the end of drilling flushing is that the residue thickness at the bottom of the hole is not greater than 20 cm after flushing and the flushing ends when the water inside the hole is clean.

5. Results and Discussion

5.1. Discussion on Grouting Quantity and Permeability. The results of the overburden consolidation grouting of #25 dam section on the right bank are shown in Table 7. The Lugeon test was not performed on the 5 m protective layer of overburden. Table 7 shows the sequence hole I in a 25 m bedrock layer unit cement injection at 83.16 kg/m, the sequence hole II cement injection at 31.57 kg/m per unit, and the cement sequence hole III cement injection at 12.92 kg/m per unit. Thus, the injection rate from the

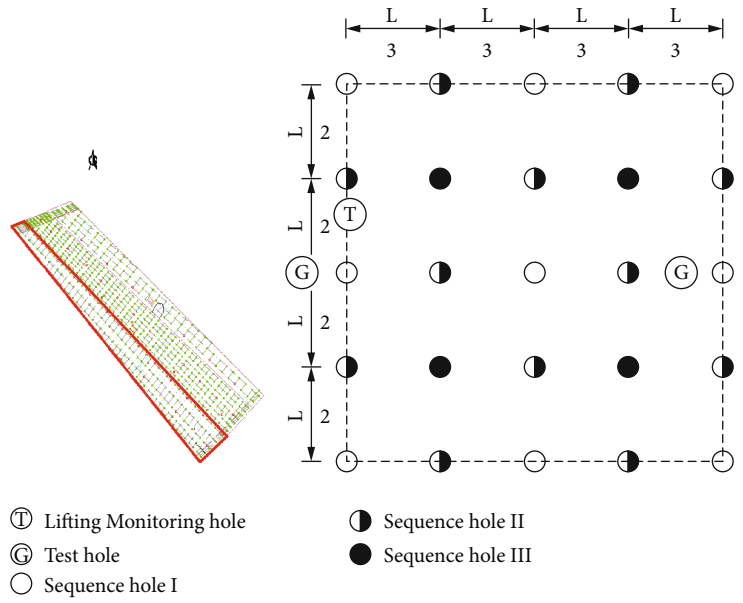

Figure 8: Schematic diagram of the grouting hole layout.

Table 7: Consolidation grouting results of the #25 dam section.

Hole	Number of holes	Grouting penetration (m)	Cement injection (kg)	Unit injection (kg/m)	Average permeability (LU)	Note
I	56	140.9	13799.2	97.94	/	5 m protective layer
II	97	270.1	4204.9	15.57	/	
III	40	127	70.2	0.55	/	
Total	193	538	18074.3	33.6	/	
I	59	1475	122658.5	83.16	23.24	25 m bedrock
II	101	2525	79721.8	31.57	9.05	
III	43	1075	13890.54	12.92	3.84	
Total	203	5075	216270.84	42.61	11.41	

sequence hole I to the sequence hole II decreases by 37%, while the grouting quantity from the sequence hole II to the sequence hole III decreases by 40.9%. As shown in Figure 9, the amount of cement injection per unit decreases significantly, which conforms to the rule of a decreasing amount of grouting per unit, indicating that cracks are effectively filled and that the grouting process has a good effect. A Lugeon test was carried out on the grouting hole before grouting of this 25 m unit of bedrock. The data in Table 8 shows that the 25 m bedrock layer averages a 23.24 LU permeable rate at the sequence hole I, averages a permeable rate of 9.05 LU at the sequence hole II, and averages a permeable rate of 3.84 LU at the sequence hole III and decreases in grouting quantity of 38.9% and 42.4%, respectively. As shown in Figure 9, the unit permeable rate decrease from the sequence hole I to the sequence hole III also explains that the rock voids were effectively filled, blocking the rock seepage pore channels and reducing the permeable rate. The gradual decrease in water permeability and cement injection per unit amount before grouting indicates that the

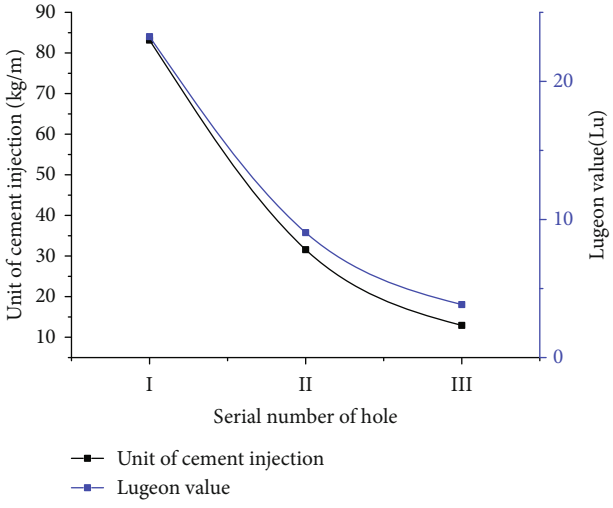

Figure 9: Trend chart of units of cement injection and Lugeon unit.

Table 8: Variation in wave velocity before and after grouting.

Before/after grouting	Velocity range (m/s)	Average minimum (m/s)	Average maximum (m/s)	Average velocity (m/s)	Statistical points
Before	3333~5970	4528	5269	4980	2105
After	3448~6061	4889	5491	5345	1253

overburden consolidation grouting method is suitable for the grouting of columnar basalt.

5.2. Discussion on Lugeon Test. The Lugeon test can directly reflect the permeability of a stratum, which is the basis for judging the stratum in the early stage of the grouting project. According to the Chinese standard DL/T5148-2012 Lugeon test (Technical Specification for Cement Grouting Construction of Hydraulic Structures), the test pressure is 80% of the grouting pressure of the corresponding section and is no more than 1.0 MPa. The Lugeon test calculation formula is shown in

$$q = \frac{Q}{PL}, \tag{1}$$

where q is the permeability of the test section, Lu; Q is the pressure inflow, L/min; P is the total pressure acting on the test section, MPa; and L is the length of test section, m.

By comparing the test data of the test hole before grouting and quality inspection of the Lugeon value after grouting, the variation parameters of the permeability of the dam foundation rock layer are obtained, and the grouting effect is evaluated. Lugeon tests were carried out on 17 test holes before grouting. The water pressure in 89 sections was greater than 4.5 LU in 69 sections, and the permeation rate over 3 LU accounted for 68.5% of all the test holes. A Lugeon test and inspection were carried out 7 d after the end of grouting. During this process, 10 test holes, with a hole depth of 25 m (excluding the 5 m protective layer) and 5 m section, were randomly drilled to conduct the Lugeon test, and a total of 50 sections of pressurized water were considered. After grouting, the Lugeon test results were collected and are shown in Figures 10 and 11. All 50 sections have Lugeon values less than 3 LU, the average permeability of the G1-G5 test hole is less than 1.5 LU, and the average permeability of the G5-G6 test hole is less than 1.2 LU. After grouting, the permeation rate of the pressurized water test section at all the inspection holes should not be greater than 3 LU. The permeability is obviously reduced, and the antiseepage effect is greatly improved. Effect analysis shows that the weight of the 5 m thick overburden can stop the fracturing and lifting of the base surface caused by high-pressure fluid. The grouting pressure is very important for the formation stability. A low-pressure grout cannot fill rock fractures effectively, and only a high-pressure grout can fill small cracks. The weight of a 5 m thick slurry seal overburden can provide an effective force to meet the required grouting pressure to limit formation disturbance. Cracks are effectively filled under high pressure, which leads to a decrease in permeability and a significant improvement in the antiseepage and consolidation effects.

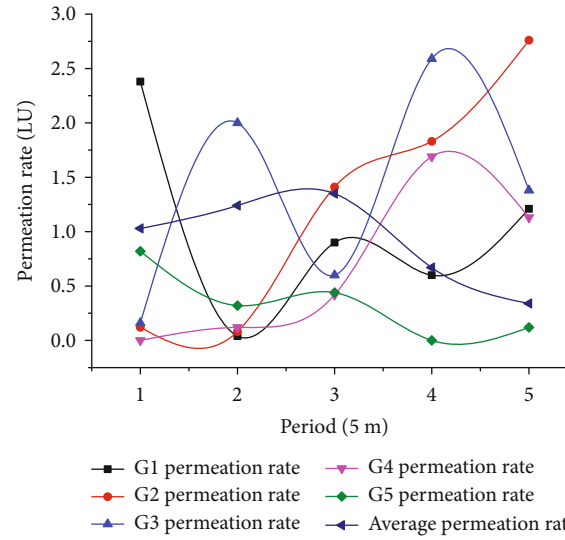

Figure 10: Permeability of test hole G1-G5.

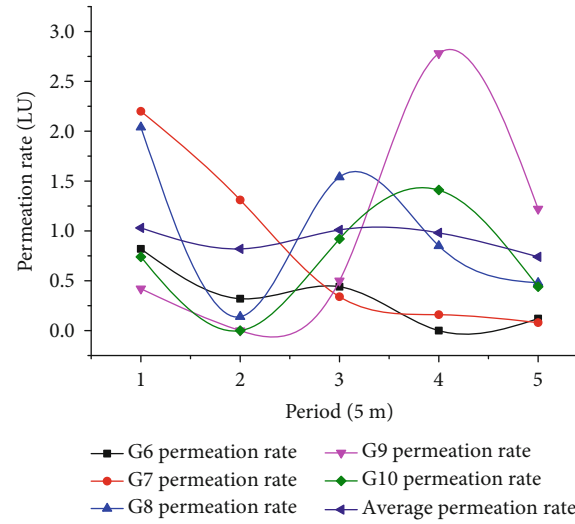

Figure 11: Permeability of test hole G6-G10.

5.3. Discussion on Geophysical Prospecting Test. Acoustic testing is the basis for determining the correlation between the physical and mechanical parameters of a rock mass and provides effective parameter indexes for detecting the influence of blasting excavation on rock engineering; this testing considers the weathering coefficient, integrity coefficient, anisotropy coefficient, faulting, karstification, and other geological defects. The higher the wave velocity is, the better the rock physical and mechanical properties and rock integrity.

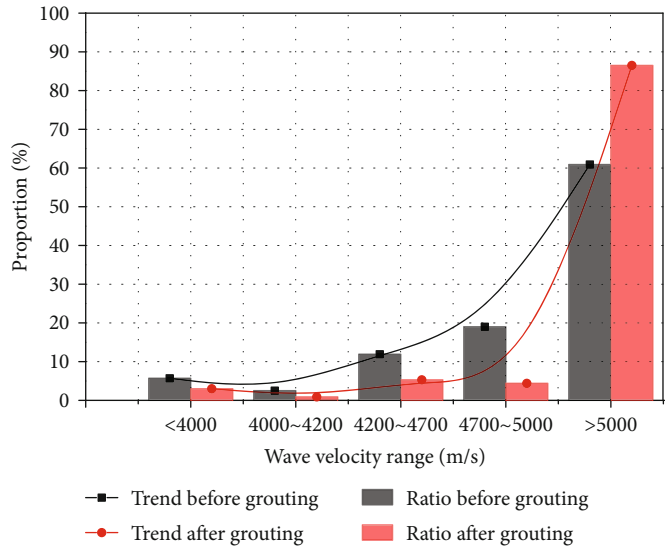

Figure 12: Velocity distribution before and after grouting for the #25 dam section.

Table 9: Comparison of the deformation modulus before and after grouting.

Before/after grouting	Deformation modulus range (GPa)	Average minimum (GPa)	Average maximum (GPa)	Average deformation modulus (GPa)	Statistical points
Before	5.50~13.42	7.46	9.9	8.56	75
After	5.73~13.26	7.69	10.41	8.71	48

The acoustic testing equipment used in this study is a rs-st01c sonic instrument produced by Wuhan Yanhai Engineering Development Co. The acoustic testing is conducted on test holes before grouting and inspection holes after grouting. Through comparison of the test results before and after grouting, rock integrity change parameters are obtained, and the grouting quality is analyzed. Grouting inspection hole drilling is conducted 14 days after the completion of grouting. The wave velocity of fresh intact rock is an important parameter for calculating the integrity coefficient and the weathering wave velocity ratio of a rock mass.

According to the early indoor rock acoustic test statistics, the average wave velocity of brecciated lava is 4272 m/s, and the range for basalt is 5132~574 m/s. Table 8 shows the changes in the wave velocity before and after grouting. Table 8 shows that the wave velocity of the 17 test holes before grouting ranges from 3333 m/s to 5970 m/s, with an average wave velocity of 4980 m/s. After grouting, 10 random inspection holes are drilled for acoustic testing, with a range of wave velocity from 3448 m/s to 6061 m/s and an average wave velocity of 5345 m/s. According to the average wave velocities of 4980 m/s before grouting and 5345 m/s after grouting, the average rate of increase in the wave velocity after grouting is 7.3%. Moreover, the wave velocity range, the mean minimum velocity, and the mean maximum velocity all increase due to grouting, indicating that the rock integrity is improved. According to Figure 12, before grouting, the wave velocity proportion ≥ 4700 m/s is 79.9% and that <4200 m/s is 8.2%. After grouting, wave velocity ≥ 4700 m/s accounted for 94.8% and that <4200 m/s accounted for 1.4%. According to the acoustic inspection standard of the dam foundation rock mass stipulated in the design document, more than 90% of the columnar basalt should have a velocity greater than 4500 m/s, and less than 5% should have a velocity less than 4200 m/s after grouting to meet the inspection standard of a rock mass. Figure 12 shows that for an initial velocity greater than 5000 m/s, the wave velocity ratio of grouting increased by 25.6%; for an initial velocity less than 5000 m/s, the wave velocity of the filling ratio dropped by approximately 50%; and for an initial velocity less than 5000 m/s, the wave velocity decreased after grouting. Due to the filling of the fractures, fissures, and fault zones, the wave velocity increased, showing that the effect of grouting is obvious.

The deformation modulus is an important parameter of rock mass for stability theory analysis and engineering design. In particular, under the condition of deformation as a stability control standard, the determination of the deformation modulus directly determines the results of a deformation stability analysis. A Probex-1 dilatometer produced by the Canadian company Roctest is used for the deformation modulus testing via field hole entry testing. The dilatometer indirectly measures the radial deformation of a rock mass through flexible pressurization. Seven test holes were tested to identify the variation in deformation modulus before grouting, and 5 test holes were tested after grouting. The data are shown in Table 9. Table 9 shows that the average deformation modulus before grouting is 8.56 GPa and the average

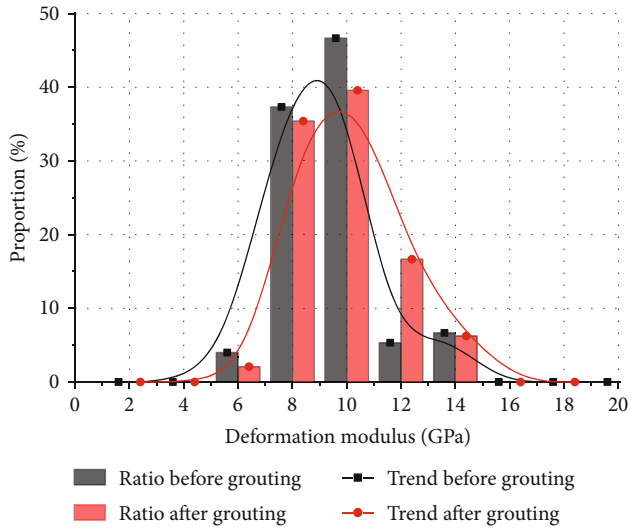

Figure 13: Distribution of deformation modulus after grouting.

deformation modulus after grouting is 8.71 GPa; the average deformation modulus after grouting is 1.7% higher. As shown in Figure 13, the ratio of the deformation modulus increased by 11.4% to 12 GPa after grouting, and the ratios of 8 and 10 GPa decreased by 1.9% and 7.1% compared to that of 6 GPa, respectively. The improvement in the rock deformation modulus of the dam foundation indicates that the resistance stress value of the rock mass increases and the strain decreases, which indirectly indicates that the physical properties of the rock are improved and that the mechanical properties are enhanced. However, the deformation modulus of the stratum after grouting increased to 12 GPa. The analysis shows that the rock integrity is relatively good because the deformation modulus data before grouting concentrate in the range of 8~10 GPa, so the increase in the modulus after grouting is relatively small.

5.4. Discussion on Stratum Lifting Monitoring. The lifting monitoring value is an important control index to reflect the influence of grouting on a stratum during construction. Two lifting observation holes are arranged in this test area. The hole depth, 3 m, is deeper than the consolidation grouting hole, and the diameter is Φ91 mm. Measuring instruments are embedded for monitoring, and they include a measuring pipe (Φ25 mm) and an external tube (Φ73 mm). The lower end is anchored into the concrete, the local layer is lifted, the inner tube will be displaced, and the dial gauge will record the data. Manual lifting monitoring data recording is adopted for lifting monitoring, and the reading is recorded every 5~10 min. Lifting deformation is monitored and recorded during grouting and water compaction, and the bedrock lifting of no more than 200 m is allowed. During grouting, the lifting deformation value varies from 11 to 31 μm, which does not exceed the specification design requirements. Figure 14 shows a manual lifting monitoring meter embedded in the field.

5.5. Discussion on Rock Core and Hole Camera. After grouting, cores are taken from 10 test holes, some of which are shown in Figure 15. Figure 15 shows that the rock cracks are effectively filled by the consolidated slurry and the grouting materials are tightly bonded to the surrounding rocks, with an obvious phenomenon of complete consolidation. There is no collapse observed during drilling, and intact core samples are collected, up to 1.2 m long, as shown in Figure 15.

A JL-IDOI panoramic imager produced by Wuhan Himalaya Digital Imaging Technology Co. is used to image the test holes, as shown in Figures 16 and 17. Figure 16 shows the typical fissure structure of some test holes before grouting. Figure 16(e) shows that some fissures have width of up to 10 cm. Some of the rocks are also filled with quartz. The rock of dam foundation contains horizontal fissure, vertical fissure, and broken zone. Figure 17 shows typical examples of consolidated slurry filling in some test holes after grouting. Figures 17(a) and 17(b) show that both the steeply inclined fissures and holes are filled effectively, and consolidated slurry filling, as well as microfissures and broken zones, can be seen in Figures 17(c)–17(f).

6. Field Application

6.1. Construction Plan. Overburden grouting is used for the consolidation grouting of dam foundation sections #19~#25 (below the 590 m platform), while no cover is used for the consolidation grouting of dam section #25 (above the 590 m platform)~#31. The grouting method is still overburden consolidation grouting, the spacing of the rows of holes is 3.00 m × 3.00 m and 2.00 m × 2.00 m, and the depth of a rock entry hole is generally 15.00~30.00 m; the development site of the structural plane and the surrounding area of the curtain line are appropriately deepened locally. Construction process: lifting monitoring hole → test hole before grouting → sequence hole I → sequence hole II → sequence hole III → test holes after grouting. The overall construction process of dam sections #19~#25 is shown in Figure 18. Slurry production stations and slurry storage stations are arranged on the upstream side of the dam foundation and connected to the grouting field by pipeline extraction.

6.2. Cement Injection Quantity and Water Permeability. The right bank dam foundation elevation, 590 m below the overburden consolidation grouting, is used to determine the injection quantity. Sequence hole I grouting is 25915 m; sequence hole II grouting is 50690 m; sequence hole III grouting is 25045 m; sequence hole IV (encryption) filling grouting hole is 49690 m. The average permeability of grouting holes in each sequence of the dam foundation and the unit cement injection amount are shown in Figures 19 and 20.

7. Conclusions

Overburden consolidation grouting has solved the characteristics of easy relaxation, strength reduction, and permeability increase of columnar jointed basalt after unloading. Moreover, overburden consolidation grouting improves the integrity and impermeability of the dam foundation rock quality and has the following advantages:

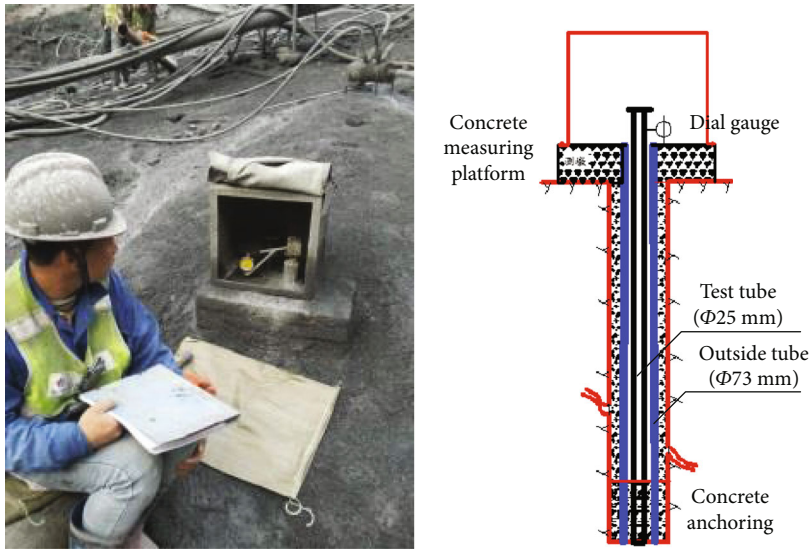

Figure 14: Field lifting monitoring.

Figure 15: Test hole core sampling.

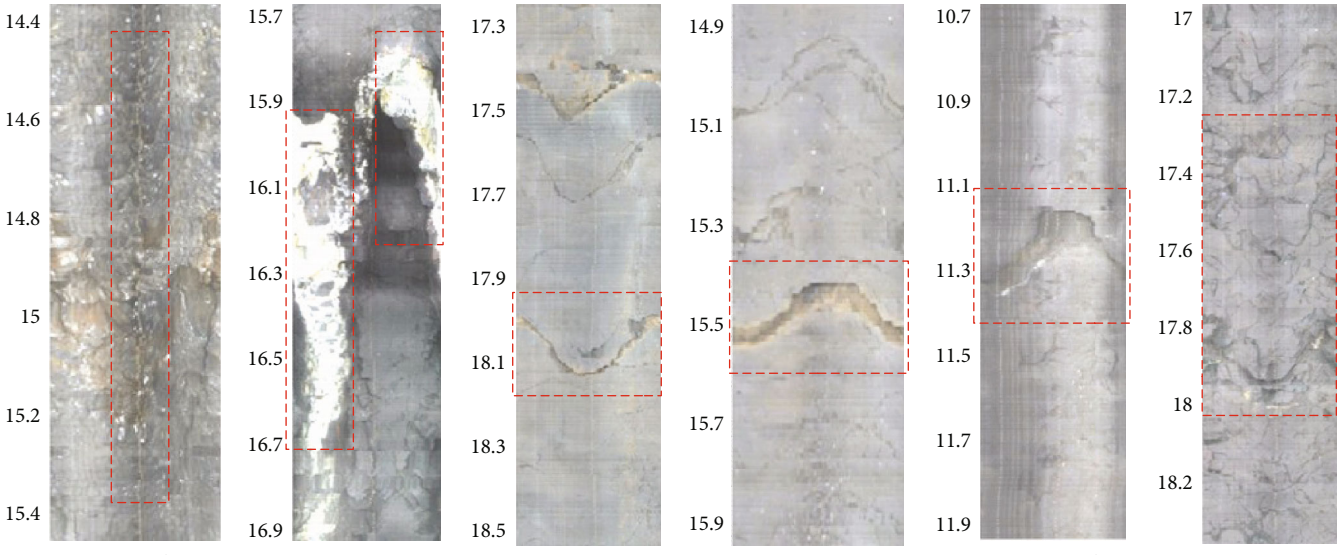

Figure 16: Typical structures in some test holes before grouting.

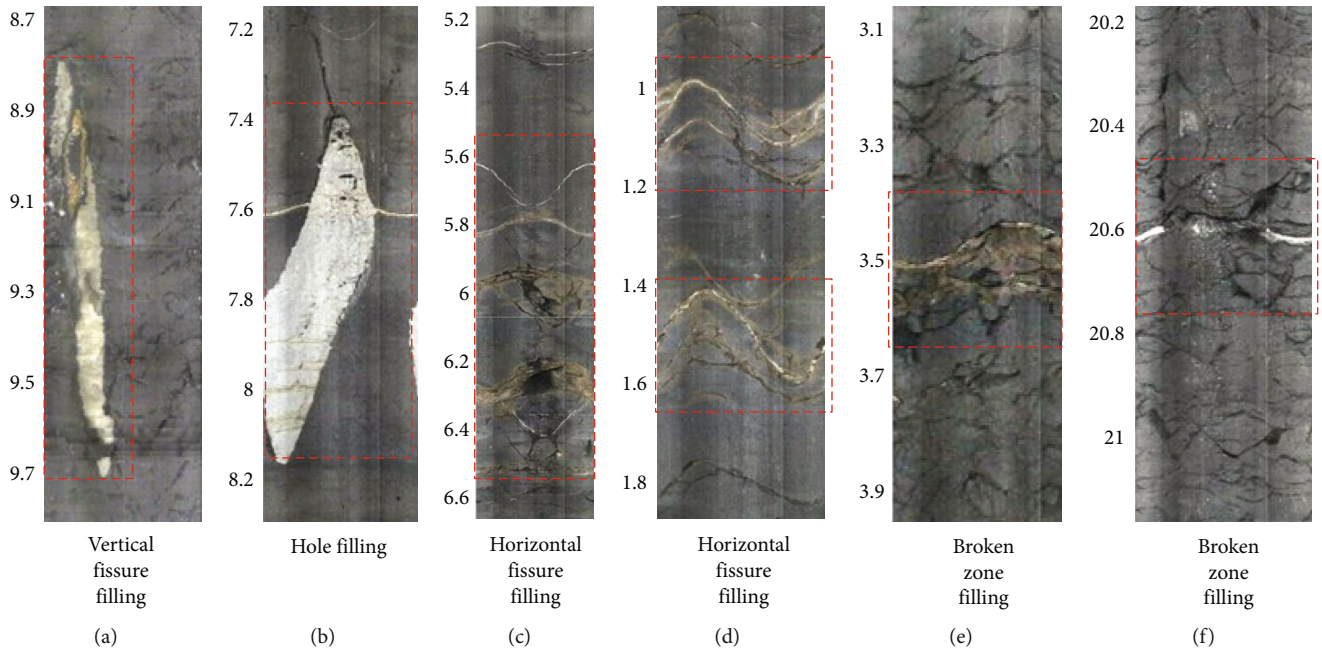

Figure 17: Typical cement filling in test holes after grouting.

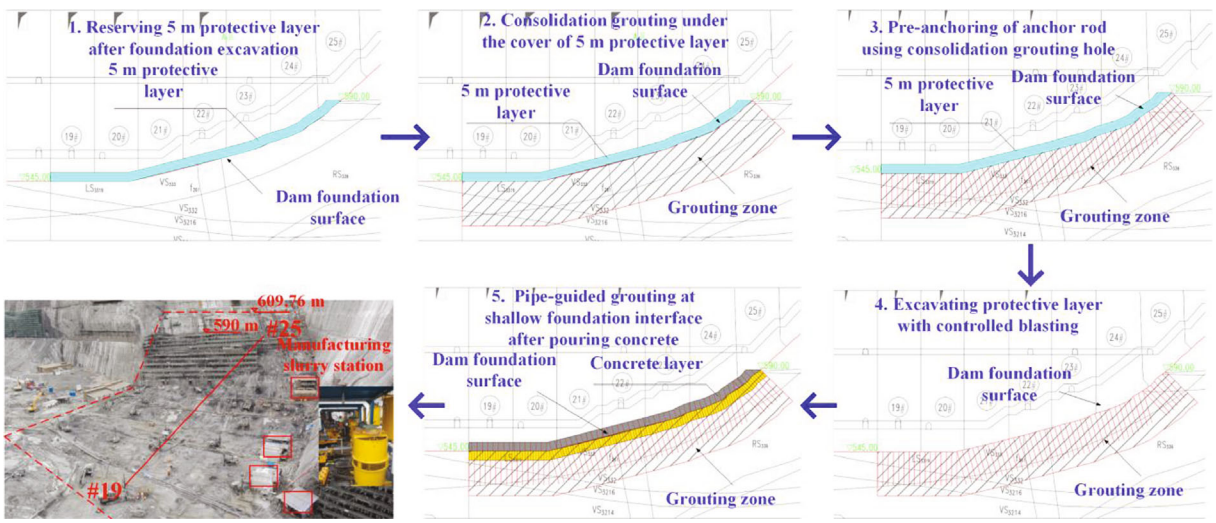

Figure 18: Overall construction process diagram of consolidation grouting at the right bank dam foundation.

(1) Overburden consolidation grouting solves the influence of the columnar jointed basalt, limits the relaxation of the surface layer, and strengthens the initially poor integrity of the rock mass. The insufficient bearing capacity of the dam foundation is strengthened, which is caused by deformation. Overburden consolidation grouting through the reserved 5 m protective layer and anchor bar pile after grouting reduces the effects of the columnar joints in the basalt. After the protective layer is excavated, the relaxation effect of the columnar basalt surface is reduced by pipe grouting. Grouting technology is suitable for the geological characteristics of columnar basalts. After consolidation grouting construction, the postgrouting inspection indicates that the grouting effect meets the requirements of the bearing capacity of an arch dam foundation, providing a successful new consolidation grouting technology

(2) The consolidation grouting effect of an overburden is considerable. There are 10 test holes with a total of 50 sections, and the 49 sections of the Lugeon test are all less than 3 LU. After grouting, the previous rate of the pressurized water test section with more than 99% check holes is no more than 3 LU. The average wave velocity before grouting is 4980 m/s, while the average wave velocity after grouting is 5345 m/s, and the increase in wave velocity due to grouting is 7.3%.

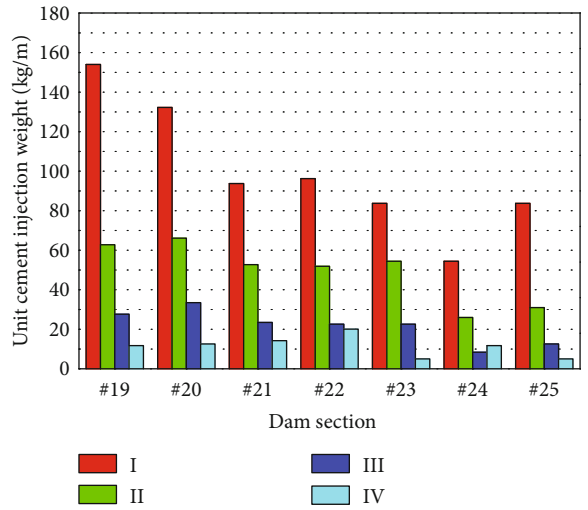

Figure 19: #19~#25 dam section consolidation grouting of hole: unit cement injection weight.

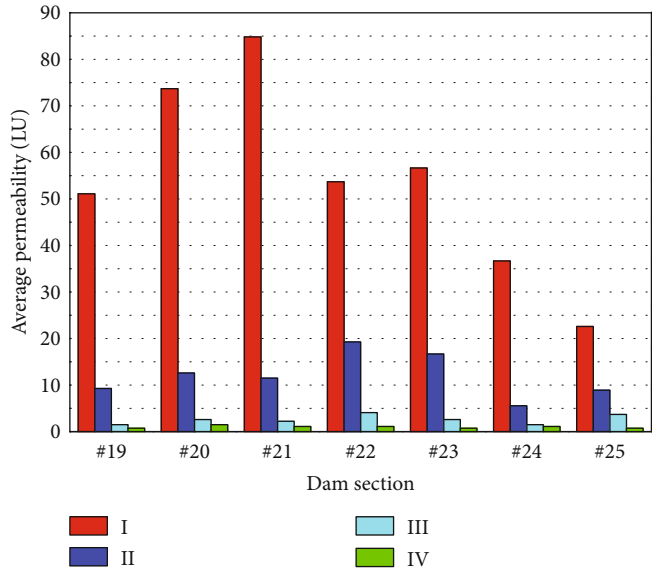

Figure 20: #19~#25 dam section consolidation grouting of hole: average permeability.

The average deformation modulus before grouting is 8.56 GPa, and the average deformation modulus after grouting is 9.9 GPa. The average deformation modulus after grouting is 13.5% higher. The lifting monitoring value ranges from 11 to 31 μm and does not exceed the specification design limit of 200 μm. The core samples were retrieved intact and are up to 1.2 m long. In addition, there is less seepage during grouting. Compared with the concrete cover consolidation grouting, this new approach can avoid the adverse effects of drilling damage to the embedded monitoring instrument and cooling water pipe and determine the influence of grouting lifting on the quality of concrete, so it has a good applicability

(3) Overburden consolidation grouting solves the problem of continuous construction. After the excavation of the top surface of the protective layer, the overburden with consolidation grouting has a large area of construction resource organization. The construction is completed before concrete pouring, and the construction resources are in place at one time. After consolidation grouting, infill grouting (as required), and test hole construction, only a small amount of resources is needed for shallow inspection after excavation of the rock protection layer. Compared with the resources of consolidation grouting for concrete cover, the waste of construction resources is avoided, and the construction efficiency is high

(4) This new process is applied to the #19~#25 dam sections of the right bank of the Baihetan hydropower station (below the 590 m platform). The successful application of overburden consolidation grouting construction technology provides a powerful reference for more dam consolidation grouting projects, which is of great significance for popularization of this approach

Data Availability

The data used to support the findings of this study are included within the article.

Conflicts of Interest

The authors declare that there is no conflict of interest regarding the publication of this paper.

Acknowledgments

This study was supported by the National Natural Science Foundation of China (Grant No. 51279019). The authors are grateful to our partners Sinohydro Bureau 8 Co., Ltd., in China. The authors are also grateful to the China Three Gorges Corporation. This paper summarizes the investigation and analysis results on the columnar jointed basalt at the Baihetan arch dam over the years, which is the wisdom of all the companies and institutions participating in this project, including design, construction supervision, and research, as well as many experts and scholars both at home and abroad. We hereby express our gratitude to all the organizations and individuals involved.

References

[1] K. D. Weaver, *Dam Foundation Grouting*, ASCE Publication, 1991.

[2] P. Lin, J. Shi, P. Wei, Q. Fan, and Z. Wang, "Shallow unloading deformation analysis on Baihetan super-high arch dam foundation," *Bulletin of Engineering Geology and the Environment*, vol. 78, no. 8, pp. 5551–5568, 2019.

[3] S. Anchi, T. Mingfa, and Z. Qijian, "Study on deformation characteristics of columnar jointed basalt rock mass of Baihetan hydropower station on Jinsha river," *Journal of Rock Mechanics and Engineering*, vol. 27, no. 10, pp. 2079–2086, 2008.

[4] J. L. Smellie, I. L. Millar, P. J. Butterworth, and D. C. Rex, "Subaqueous, basaltic lava dome and carapace breccia on King George Island, South Shetland islands, antarctica," *Bulletin of Volcanology*, vol. 59, no. 4, pp. 245–261, 1998.

[5] C. J. Allegre, A. Provost, and C. Jaupart, "Oscillatory zoning: a pathological case of crystal growth," *Nature*, vol. 294, no. 5838, pp. 223–228, 1981.

[6] C. Changyan and G. Wang, "Discussion on the interrelation of various rock mass quality classification systems at home and abroad," *Chinese Journal of Rock Mechanics and Engineering*, vol. 21, no. 12, pp. 1894–1900, 2002.

[7] J. M. Degraff, P. E. Long, and A. Aydin, "Use of joint-growth directions and rock textures to infer thermal regimes during solidification of basaltic lava flows," *Journal of Volcanology and Geothermal Research*, vol. 38, no. 3-4, pp. 309–324, 1989.

[8] C. S. Haase, J. Chadam, D. Feinn, and P. Ortoleva, "Oscillatory zoning in plagioclase feldspar," *Science*, vol. 209, no. 4453, pp. 272–274, 1980.

[9] A. C. Lasaga, "Toward a master equation in crystal growth," *American Journal of Science*, vol. 282, no. 8, pp. 1264–1288, 1982.

[10] P. E. Long and B. J. Wood, "Structures, textures, and cooling histories of Columbia River basalt flows: discussion and reply: reply," *Geological Society of America Bulletin*, vol. 97, no. 9, pp. 1144–1155, 1986.

[11] A. R. McBirney and T. Murase, "Rheological properties of magmas," *Annual Review of Earth and Planetary Sciences*, vol. 12, no. 1, pp. 337–357, 1984.

[12] P. Ortoleva, *Chemical Instabilities*, D. Reidel Publishing Company, Dordrecht, 1984.

[13] D. Pollard, "Elementary fracture mechanism applied to structure interpretation of dyke," *Geological Association of Canada*, vol. 34, pp. 5–24, 1987.

[14] Q.-X. Meng, H.-L. Wang, W.-Y. Xu, and Y.-L. Chen, "Numerical homogenization study on the effects of columnar jointed structure on the mechanical properties of rock mass," *International Journal of Rock Mechanics and Mining Sciences*, vol. 124, article 104127, 2019.

[15] Q. Fan, Z. Wang, J. Xu, M. Zhou, Q. Jiang, and G. Li, "Study on deformation and control measures of columnar jointed basalt for Baihetan super-high arch dam foundation," *Rock Mechanics and Rock Engineering*, vol. 51, no. 8, pp. 2569–2595, 2018.

[16] Q. Fan, X. Feng, W. Weng, Y. Fan, and Q. Jiang, "Unloading performances and stabilizing practices for columnar jointed basalt: a case study of Baihetan hydropower station," *Journal of Rock Mechanics and Geotechnical Engineering*, vol. 9, no. 6, pp. 1041–1053, 2017.

[17] Q. Jiang, X.-t. Feng, Y. H. Hatzor, X.-j. Hao, and S.-j. Li, "Mechanical anisotropy of columnar jointed basalts: an example from the Baihetan hydropower station, China," *Engineering Geology*, vol. 175, no. 10, pp. 35–45, 2014.

[18] Y. Wei, M. Xu, W. Wang, A. Shi, and Z. Ye, "Feasibility of columnar jointed basalt used for high-arch dam foundation," *Journal of Rock Mechanics and Geotechnical Engineering*, vol. 3, no. 1, pp. 461–468, 2011.

[19] F. Wu, T. Liu, J. Liu, and X. Tang, "Excavation unloading destruction phenomena in rock dam foundations," *Bulletin of Engineering Geology and the Environment*, vol. 68, no. 2, pp. 257–262, 2009.

[20] Q. X. Fan, S. W. Zhou, and N. Yang, "Optimization design of foundation excavation for Xiluodu super-high arch dam in China," *Journal of Rock Mechanics and Geotechnical Engineering*, vol. 7, no. 2, pp. 120–135, 2015.

[21] D. Develay, R. J. Hagen, and R. Bestagno, "Lesotho highlands water project-design and construction of Katse dam," *Proceedings of the Institution of Civil Engineers - Civil Engineering*, vol. 120, no. 5, pp. 14–29, 1997.

[22] D. Homas and J. Thomas, "Large-scale field investigation of grouting in hard jointed rock," in *Proceedings of the 3rd International Specialty Conference on Grouting and Ground Treatment*, pp. 1628–1639, New Orleans, LA, USA, February 2003.

[23] Z. Yonggang, "Study of arch dam foundation treatment for Shapai hydroelectric power station," *Design of Hydroelectric Power Station*, vol. 19, no. 4, pp. 64–68, 2003.

[24] L. Ming and T. Shuming, "Model test and analysis of combined anchoring mechanism of active and passive anchors on fragmental structural rock cutting slope," *Technology of Highway and Transport*, vol. 6, no. 3, pp. 19–21, 2003.

[25] K. Terzaghi and MICE, "Dam foundation on sheeted granite," *Géotechnique*, vol. 12, no. 3, pp. 199–208, 1962.

[26] S. Turkmen, E. Özgüler, H. Taga, and T. Karaogullarindan, "Seepage problems in the karstic limestone foundation of the Kalecik Dam (south Turkey)," *Engineering Geology*, vol. 63, no. 3–4, pp. 247–257, 2002.

[27] K. Kikuchi, T. Igari, Y. Mito, and S. Utsuki, "In situ experimental studies on improvement of rock masses by grouting treatment," *International Journal of Rock Mechanics and Mining Sciences*, vol. 34, no. 3–4, pp. 138.e1–138.e14, 1997.

[28] M. H. Salimian, A. Baghbanan, H. Hashemolhosseini, M. Dehghanipoodeh, and S. Norouzi, "Effect of grouting on shear behavior of rock joint," *International Journal of Rock Mechanics and Mining Sciences*, vol. 98, pp. 159–166, 2017.

[29] Q. X. Meng, H. L. Wang, W. Y. Xu, M. Cai, J. Xu, and Q. Zhang, "Multiscale strength reduction method for heterogeneous slope using hierarchical FEM/DEM modeling," *Computers and Geotechnics*, vol. 115, p. 103164, 2019.

[30] Q. X. Meng, H. L. Wang, W. Y. Xu, and M. Cai, "A numerical homogenization study of the elastic property of a soil-rock mixture using random mesostructure generation," *Computers and Geotechnics*, vol. 98, pp. 48–57, 2018.

[31] J. Xu, C. Xiaolin, Z. Wei, Z. Chao, and G. Huawei, "Study on the effect of cover lifting on concrete stress during consolidation grouting," *Journal of Hydraulic Power*, vol. 10, 2016.